Biomimetic Cryptic Site Surfaces for Reversible Chemo- and Cyto-Mechanoresponsive Substrates

Jalal Bacharouche,[†] Florent Badique,[†] Ahmad Fahs,[‡] Maria V. Spanedda,[§] Alexandre Geissler,[†] Jean-Pierre Malval,[†] Marie-France Vallat,[†] Karine Anselme,[†] Grégory Francius,[‡] Benoit Frisch,[§] Joseph Hemmerlé,[⊥] Pierre Schaaf,[⊥,∥,*] and Vincent Roucoules[†]

[†]Institut de Sciences des Matériaux de Mulhouse, IS2M-LRC 7228 CNRS/Université de Haute-Alsace, 15, Rue Jean Starcky, 68057 Mulhouse Cedex, France, [‡]Laboratoire de Chimie-Physique et Microbiologie pour l'Environnement, CNRS/Université de Lorraine (UMR 7564), 405 Rue de Vandoeuvre, 54601 Villers-les-Nancy, France, [§]Laboratoire de Conception et Application de Molécules Bioactives, CNRS/Université de Strasbourg, Faculté de Pharmacie, 74 Route du Rhin, 67401 Illkirch Cedex, France, [⊥]Institut National de la Santé et de la Recherche médicale (INSERM U 1121), 11 Rue Humann, 67085 Strasbourg Cedex, France, and [∥]Institut Charles Sadron (CNRS UPR 22), 23 Rue du Loess, 67034 Strasbourg Cedex, France

ABSTRACT Chemo-mechanotransduction, the way by which mechanical forces are transformed into chemical signals, plays a fundamental role in many biological processes. The first step of mechanotransduction often relies on exposure, under stretching, of cryptic sites buried in adhesion proteins. Likewise, here we report the first example of synthetic surfaces allowing for specific and fully reversible adhesion of proteins or cells promoted by mechanical action. Silicone sheets are first plasma treated and then functionalized by grafting sequentially under stretching poly(ethylene glycol) (PEG) chains and biotin or arginine-glycine-aspartic acid (RGD) peptides. At unstretched position, these ligands are not accessible for their receptors. Under a mechanical deformation, the surface becomes specifically interactive to streptavidin, biotin antibodies, or adherent for cells, the interactions both for proteins and cells being fully reversible by stretching/unstretching, revealing a reversible exposure process of the ligands. By varying the degree of stretching, the amount of interacting proteins can be varied continuously.

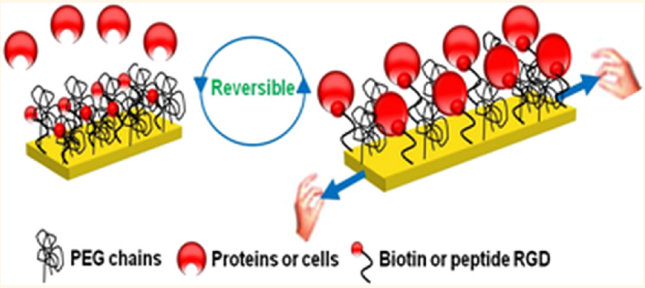

KEYWORDS: mechanoresponsive surface · mechanochemistry · cyto-responsive surface · responsive PEG brush · cryptic site surface

There are two ways by which mechanical forces can influence chemical reactions: either directly by acting on chemical bonds,[1−3] which usually requires large constraints or high energy often applied through sonication[4] (a domain now called "covalent mechanochemistry"[5]), or by mimicking nature which acts through conformational changes of proteins resulting in favoring noncovalent interactions. This ultimately leads, through a cascade of processes, to reactions involving covalent bonds. This is the case, for example, during cell adhesion where the exhibition, under stretching, of cryptic sites buried in proteins ultimately results in the formation of focal adhesions.[6−8] This second route needs much lower constraints and energy than direct action on chemical bonds.

Along this line, some of us have introduced the first example of films becoming enzymatically active under stretching[9] and more recently cyto-mechanoresponsive.[10] Both examples rely on a general strategy based on embedding active compounds in polyelectrolyte multilayers and rendering them accessible by modifying the multilayer architecture by stretching. Unfortunately, up to now, this strategy did not allow to design fully reversible systems.[10,11] The challenge to create fully reversible chemo- and cyto-mechanoresponsive films remains thus totally open. To take up this challenge, we introduce here cryptic site substrates that reproduce more closely the behavior of cryptic site proteins. The concept is schematically represented in Figure 1A.

RESULTS AND DISCUSSION

Chemo-Mechanoresponsive System. In order to create such cryptic site substrates, we adapted

* Address correspondence to schaaf@unistra.fr.

Received for review January 23, 2013 and accepted March 26, 2013.

Published online March 26, 2013
10.1021/nn400356p

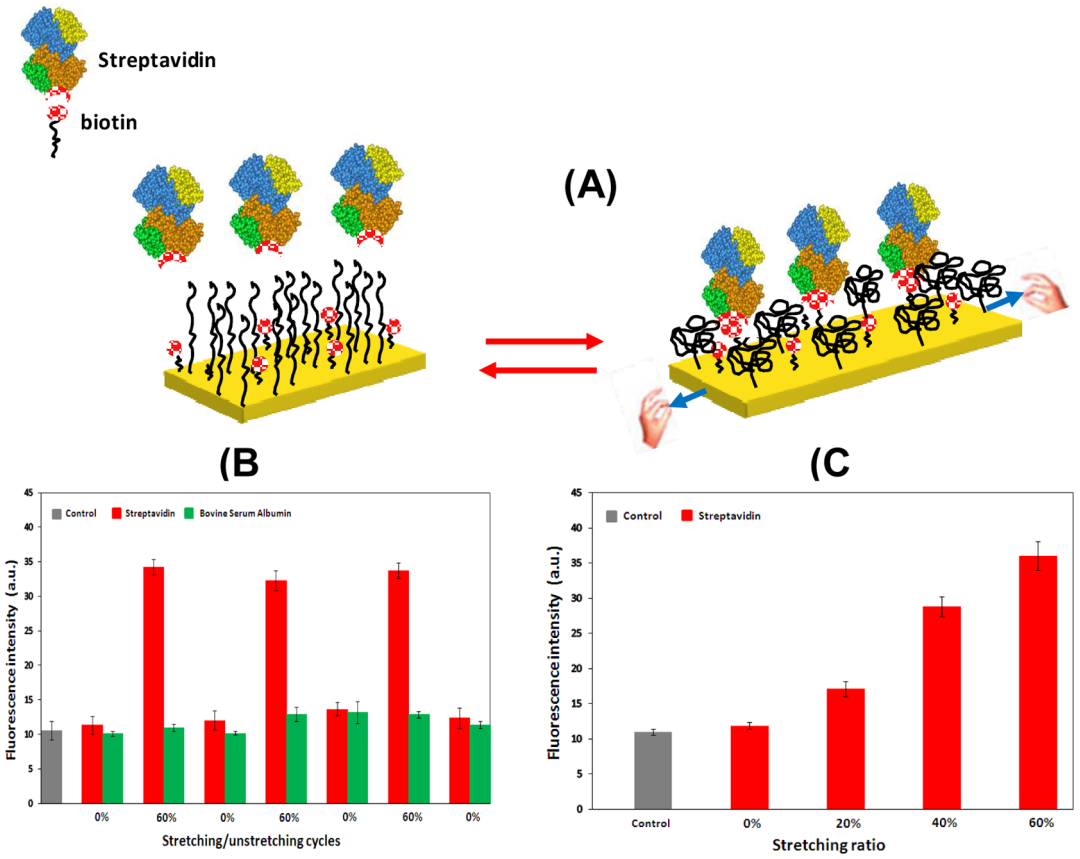

Figure 1. (A) Schematic representation of the fully reversible cryptic site mechanoresponsive surface. In the unstretched state, due to the high density of PEG chains grafted onto the substrate, the ligands are not accessible to their receptors. Under stretching, the PEG chain density decreases, rendering the ligands accessible. (B,C) Fluorescence intensity of functionalized silicone sheets measured at 520 nm by fluorescence microscopy. Before each measurement, the substrate was brought in contact with a FITC-labeled protein solution and further rinsed with buffer. (B) Evolution of the fluorescence intensity for a series of three stretching (60%)/unstretching (0%) cycles. The substrates were functionalized with PEG-2000 and biotin and brought in contact with FITC-streptavidin (red) or FITC-albumin (green). (C) Evolution of the fluorescence intensity for a substrate functionalized with PEG-2000 and biotin after having been brought in contact with a FITC-streptavidin solution at various stretching ratios: 0% (nonstretched state), 20%, 40%, 60%.

a technique first introduced by Genzer,[12] who grafted alkanethiols on an elastomeric surface under stretching to create superhydrophobic substrates. Here we use silicone substrates that are treated with anhydride maleic polymer plasma under conditions preserving the surface from cracking under stretching.[13] This operation results in the spreading of anhydride maleic groups over the elastomer substrate. In the presence of deionized water, these groups are further hydrolyzed to give a homogeneous coverage of carboxylic groups over the silicone substrate. The plasma treatment as well as all of the following surface treatments is performed under 60% uniaxial stretching of the substrate. This surface, stretched at 60%, is then brought in contact with a solution of (amino)PEG chains in the presence of ethyl(dimethylaminopropyl)carbodiimide (EDC) and *N*-hydroxysuccinimide (NHS) in PBS buffer under cloud point conditions at 60 °C for 12 h.[14,15] The PEG chains are terminated at one end by amine groups and have a molecular weight of 2000 (degree of polymerization $n = 45$). The reaction between the amine and the carboxylic groups leads to the formation of amides. After PEG grafting, the 60% stretched substrate is brought back to room temperature. The ligands are then grafted, still under stretching, on the unreacted carboxylic groups through a similar chemical grafting procedure. As ligands, we use either small PEG chains (two ethylene glycol monomers) that bear at one end biotin and at the other end an amine group (denoted as biotin) or peptides containing the RGD adhesion sequence. More details of the whole functionalization method are given in Supporting Information (SI). Subsequently, the silicone is brought back to its nonstretched state. The efficiency of PEG grafting was verified by measuring the contact angle of water which changed from 102 to 60° after plasma treatment and PEG grafting. By using fluorescence microscopy, it was also verified that this PEG-coated substrate is nonadsorbent to albumin or streptavidin and that it remains antifouling even under stretching at 60% (Figure 1 in SI). XPS analysis of the grafted surfaces indicates that the presence of nitrogen and new peaks in the C(1s) envelope at 285.3 and 286.2 eV corresponding to amide groups (Table 1 and Figure 2 in SI) confirm the covalent

binding of ethylene glycol molecules on the surface *via* amide linkages. AFM imaging reveals that the surface is totally and homogeneously covered with PEG (Figure 3 in SI). Next, we verified that the PEG/biotin-functionalized surface remains non-adsorbent at unstretched position to albumin and streptavidin. The presence of grafted biotin is proven by the high fluorescence signal observed when the substrate is stretched at 60% and brought in contact with fluorescein-functionalized streptavidin (named streptavidin). When the entire grafting procedure of both the PEG and biotin is performed at unstretched position, strong streptavidin adsorption is observed at unstretched position (Figure 4 in SI), indicating that biotin is not masked in this case by the PEG chains.

Let us now analyze the behavior of such a substrate for a series of stretching/unstretching cycles. The evolution of the fluorescence signal is represented in Figure 1B. In the absence of any fluorescent protein, one measures a background signal originating from the plasma treatment of the silicone. The substrate is then brought in contact with a solution of fluorescently labeled streptavidin or albumin (and subsequently rinsed). No increase of the fluorescence is observed in both cases as already mentioned. When this substrate is stretched at 60% and put in contact with the streptavidin solution, a strong increase of the surface fluorescence is observed after rinsing, due to the streptavidin interaction with biotin. When the same surface is brought in contact with FITC-albumin instead of streptavidin, no fluorescence increase is measured, indicating that the surface remains non-adsorbent to albumin. When the surface exposed to streptavidin comes back to its unstretched position, one recovers the background intensity, indicating that all of the streptavidin bound to biotin under stretching is expelled from the surface. This cycle is repeated three times and appears fully reversible (Figure 1B). In particular, the surface becomes each time non-adsorbent to streptavidin (and remains non-adsorbent to albumin) when returning to the nonstretched state. The reversibility is further investigated by repeating stretching/unstretching cycles 10 times outside the microscope before performing one cycle under the fluorescent microscope (Figure 5 in SI). We verified that after 10 streching/unstretching cycles the silicone recovers its initial length within 10%. Strong fluorescence under stretching and full reversibility are again observed, showing the robustness of our system. These results thus clearly show that we have created a functionalized surface that becomes specifically interactive to streptavidin under stretching and that the process is fully reversible. All of the results reported so far were performed with PEG-2000 chains.

We also performed experiments with shorter chains, PEG-750, corresponding to 17 ethylene oxide monomers instead of 45 for PEG-2000. For PEG-750, one observes a strong fluorescence increase when the films are brought in contact with the streptavidin solution in the nonstretched state. When these films are stretched at 60%, the increase in fluorescence is small compared to the signal in the nonstretched state (Figure 6 of SI). This indicates that most of the grafted biotin groups are accessible to streptavidin under nonstretched conditions and that the proportion of groups that become accessible exclusively under stretching is small compared to the total number of grafted biotin groups. This might be due to the following reason: the short (n = 17) or long chains (n = 45) grafted on the stretched surface should be rather globular due to the fact that grafting takes place under cloud point conditions. After PEG grafting, there remain unreacted carboxylic groups on the surface that can be further functionalized with biotin molecules. This is attested by the presence of biotin groups as observed through streptavidin interaction. When the substrate is relaxed, the PEG-2000 (n = 45) chains hide the biotin groups which become inaccessible to streptavidin. For the shorter chains (n = 17), the density of grafted chains on the substrate can be higher. This leads to a decrease of unreacted carboxylic groups and in turn to a smaller amount of grafted biotin. This is corroborated by the diminished fluorescence signal compared to the PEG-2000 experiments when the surface is exposed to the streptavidin solution under stretching. Alternatively, the smaller PEG size should also reduce the efficiency of hiding the biotin groups in the nonstretched state. This is confirmed by the large fluorescence in the nonstretched state and by the small fluorescence increase after stretching. All of the remaining experiments were performed with PEG-2000.

Next, we investigated the effect of the stretching degree on the interaction with streptavidin (Figure 1C). The surface fluorescence due to attached streptavidin regularly increases as the stretching degree is increased up to 60%. This can be due to a continuous unmasking of the ligands as the stretching degree is increased to a regular increase of the biotin/streptavidin binding constant because of a decrease of the lateral pressure exerted by the PEG chains on streptavidin as the stretching degree increases or to both effects simultaneously.

To answer this question, force AFM experiments were performed. Streptavidin was grafted on the cantilever which was approached to the functionalized silicone substrates up to an applied force of about 500 pN. The rupture forces during retraction were then measured for a given retraction rate (2000 nm/s). Each force distribution originates from 600 force curves taken all over the substrate by using a single AFM-functionalized tip. At the beginning of each experiment, force curves were measured on a surface entirely covered with biotin. The surface was then changed, and the experiments were performed on the substrate of interest at different stretching degrees (from 0 to 60%). At the end of the series of experiments,

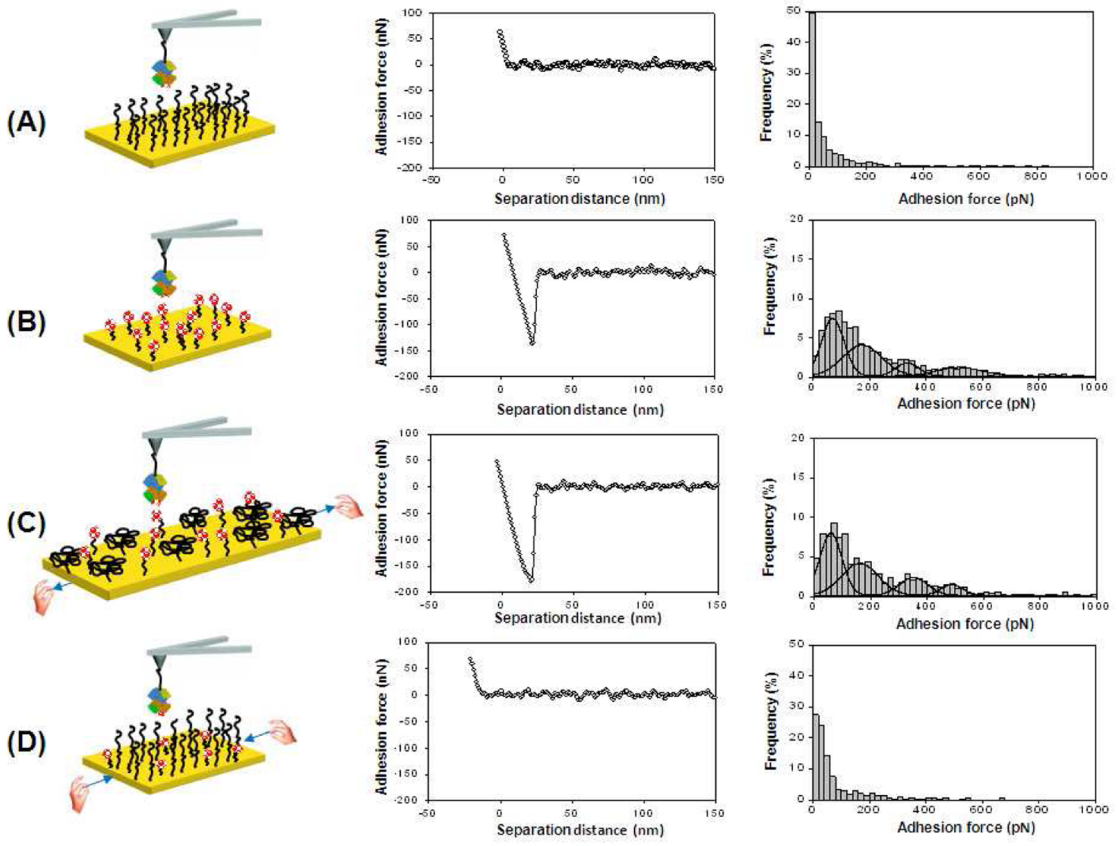

Figure 2. AFM force distributions between streptavidin grafted cantilever and (A) substrate functionalized with PEG-2000 under stretching, (B) substrate functionalized with biotin, (C) substrate functionalized under stretching with PEG and biotin; the substrate was stretched at 60% and (D) the same PEG/biotin-functionalized substrate returned to its nonstretched state. The second column represents typical force−retraction curves corresponding to the maximum of occurrence. The third column represents the histograms of the last rupture forces. The histograms corresponding to (B) and (C) are composed of four components centered on (peak 1) 69 ± 39 pN, (peak 2) 174 ± 69 pN, (peak 3) 334 ± 41 pN, (peak 4) 517 ± 79 pN for the substrate covered with biotin (B), and (peak 1) 58 ± 38 pN, (peak 2) 161 ± 65 pN, (peak 3) 351 ± 50 pN, (peak 4) 487 ± 39 pN for the substrate functionalized with PEG-2000 and biotin and stretched at 60% (C).

we performed again the experiment on a surface entirely covered with biotin in order to verify that the force curves are similar to those obtained at the beginning of the experiments. This allows us to verify that the functionalized streptavidin cantilever was not altered during the experiment. We independently functionalized three AFM tips and performed three independent sets of experiments for each experimental condition in order to verify the reproducibility (see section 11 in SI). On all measurements, we obtained differences between the adhesion force values that were generally lower than 10−15%. Further details about experimental procedure are given in SI. When the substrate was exclusively covered with biotin, the rupture force distribution was broad, ranging up to 600 pN with a multimodal distribution (Figure 2B). The first peak corresponds to a mean force of 69 ± 39 pN, while the other three correspond to about 174, 334, and 517 pN. The first value is found in good agreement with literature,[16] whereas the three last values can be attributed to multiple biotin−streptavidin interactions. When the substrate is exclusively covered with PEG, the most probable force is very low (20 pN, Figure 2A) in the range of the noise taken from force curve baseline, indicating the absence of interaction between the PEG substrate and the AFM tip. Next, experiments were performed on PEG/biotin substrates at 20, 40, and 60% stretching degrees (Figure 7 in SI). At a stretching degree of 20%, the force distribution resembles that at unstretched position, yet with a tail that extents toward 100−200 pN. At stretching degrees of 40 and 60%, the force distribution closely resembles that of a substrates covered entirely with biotin (Figure 2B). It is again characterized by a multimodal distribution. The values of the forces around which the peaks are centered are given in Table 2 in SI. The forces of the different peaks are on the same order for the surface entirely covered with biotin and the PEG/biotin surfaces stretched at 40 and 60%. Moreover, as the stretching degree increases, the amplitudes of the peaks centered around 360 and 500 pN increase at the expense of the first two peaks. This indicates that increasing the stretching degree mainly leads to a continuous unmasking of the biotin groups. The shift of the force distribution toward

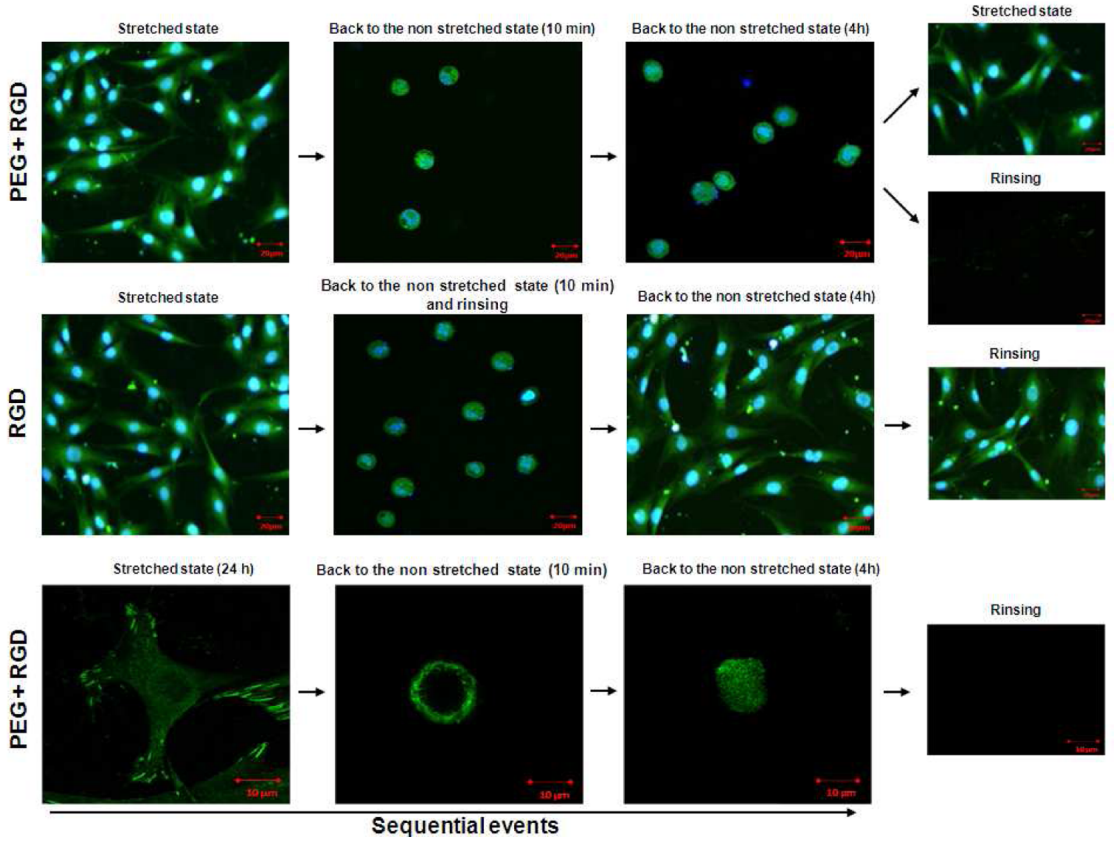

Figure 3. Confocal optical microscopy of human F/STRO-1+ A osteoprogenitor cells deposited on PEG/RGD and RGD-functionalized silicone substrates. Column 1: cells deposited on the substrates stretched at 60% during 4 h for cell phenotype observation (line 1 and 2) and during 24 h to visualize focal adhesions (line 3). Column 2: 10 min after the substrates were suddenly brought back to the nonstretched state, the RGD substrate was rinsed with buffer before the image was taken. Column 3: These substrates were left in the nonstretched state for 4 additional hours. Column 4: The PEG/RGD-functionalized substrate was then stretched again at 60% and left for 4 h (upper image of line 1 and image of line 2 (RGD)), or it was rinsed with buffer (lower image of line 1 or image of line 3 (PEG+RGD)). In this latter case, all cells were removed from the substrate due to rinsing. For imaging purposes, the F/STRO-1+ A cell nuclei were labeled with Hoechst and cell bodies with CFDA'SE (lines 1 and 2) or cells were transfected with talin-GFP to visualize focal adhesions (line 3).

100−200 pN observed at 20% stretching compared to that at unstretched position must correspond to the appearance of a peak centered at around 170 pN that overlaps with the low intensity peak tail already observed at the unstretched position or in the absence of biotin. Next, AFM experiments were performed successively on a 60% stretched PEG/biotin substrate (Figure 2C) and on a nonstretched PEG/biotin substrate (Figure 2D). Returning to the nonstretched state, one recovers the same force distribution and the same mean rupture force as on a substrate exclusively covered with PEG (Figure 2A). This proves that, by returning to the nonstretched state, the biotin groups are again hidden in the PEG brush so that the exhibition of streptavidin under stretching takes place in a fully reversible manner.

The biotin/streptavidin interaction is one of the strongest known in biology with a dissociation constant $K_d \sim 10^{-14}$ M.[16] One could thus argue that such a very strong bonding is required to overcome eventual lateral repulsions generated by the PEG brushes when the substrate is stretched which would restrain our concept to the biotin/streptavidin system. To exclude this latter hypothesis, we used anti-biotin antibodies which exhibit a weaker affinity with biotin as receptors. The dissociation constant of the antigen−antibody complexes is known to be on the order of 10^{-9} M,[17] 5 orders of magnitude higher than that corresponding to biotin/streptavidin. The biotin/anti-biotin interactions are again promoted under stretching, and the process appears again to be reversible (Figure 8 in SI).

The question that remains open is how such a strong bond as biotin/streptavidin can be ruptured when the system returns from a stretched state to unstretched position. We propose that, when returning to the nonstretched state, PEG chains exert lateral pressure on streptavidin which then changes conformation. Such conformational changes strongly affect the biotin−streptavidin interaction, streptavidin being ultimately released from the surface.

Cyto-Mechanoresponsive System. Our concept allows also creating cyto-mechanoresponsive films. For this purpose, we use the aforementioned functionalization procedure, but instead of grafting biotin, we graft RGD peptides which are known to be cell adhesion

ligands.[18,19] The goal is to verify that such a substrate is not cell adherent at unstretched position and becomes cell adherent under stretching *in a reversible manner*. Such a behavior would then be close to that of fibronectin that exhibits cryptic sites under stretching.[20] The experiments were carried out with human F/STRO-1+ A osteoprogenitor cells. We first verified that, in the absence of RGD, the substrates covered exclusively with PEG chains remained non-adherent to cells even under stretching (Figure 9 in SI). In the presence of RGD, we observed that the substrate is non-adherent to cells at unstretched position and becomes adherent when stretched at 60%. Statistical analysis of this behavior is given in Figure 10 of SI, where areas and aspect ratios of cells are compared on nonstretched and stretched substrates. In addition, cells that adhere for 4 h under stretching are released from the substrate, which becomes again cell non-adherent when it is returned in the nonstretched state. Finally, when this substrate is stretched again, it becomes again cell adherent. The results are summarized in Figure 3. They demonstrate that the ligand exposure/masking process by stretching/unstretching the substrate is fully reversible.

To obtain more details about the cellular mechanisms, we concentrated on focal adhesions. Talin is a well-known protein which interacts with vinculin and integrins in focal adhesion complex of cells[21] that anchor the cells to their substrates. Cells transfected with talin-GFP show strong condensate patches of fluorescent talin at their periphery on stretched PEG-RGD substrates (see Figure 3). This observation proves that cells are able to construct some specific focal adhesions on stretched PEG-RGD substrates. When the PEG-RGD substrates are brought back to unstretched position, only a few cells remain on the surface after 10 min. These remaining cells adopt a round shape and present some disorganized peripheral talin demonstrating that focal adhesions are detached. After 4 h, talin proteins appear diffused over the whole cell body and no longer organize in focal adhesions. A single micropipet flow on these round cells is sufficient to remove them completely from the surface. These results clearly demonstrate that cells form focal adhesions in the stretched state and that returning to the nonstretched state destroys the focal adhesions to the hiding of RGD peptides.

To ensure full reversibility of the processes, one has to verify that by returning abruptly to the nonstretched state after adhesion on the stretched substrate, there remain no proteins or extracellular matrix on the surface left by the cells during the sudden stretching release. If this would not be the case, deposition of new cells on the nonstretched substrate that was initially covered by adherent cells in the stretched state would lead to at least partial adhesion of the newly deposited cells. This is not the case: all newly deposited cells remain in a non-adherent characteristic round shape on the unstretched substrate. Moreover, if the release of stretching would lead to cell damage, cells would not remain viable. Yet, if the surface is stretched again, all cells that adhered on the surface under stretching and remained deposited on top of the nonstretched surface (in a non-adherent state in the absence of flow over the surface) after releasing the stretching do adhere again (Figure 3, line 1, column 4, stretched state). Cell detachment by substrate retraction thus seems to restore the initial configuration of the substrate, and the cyto-responsive process appears to be thus fully reversible.

Finally, if the cells are deposited on a surface entirely covered by RGD moieties without any PEG chain to prevent adhesion, adhesion is strong in the stretched and nonstretched state. When cells adhere in the stretched state and the stretching is suddenly released, the cells adopt immediately a round shape but cannot be removed by rinsing (Figure 3, line 2 (RGD)). They then rapidly spread again, and after 4 h, they reached again a spreading state similar to that of the initial stretching. When this surface was flushed with a micropipet flow, cells remained adherent on the surface (Figure 3, line 2, column 4 (rinsing)).

Our cell studies relative to focal adhesions were performed for cell adhesion times up to 24 h. During this time, each cell had already synthetized some extracellular matrix but remained removable after release. It is thus anticipated that our concept be extendable to cell sheets when cells reach confluence. Yet this has to be thoroughly investigated but lies out of the scope of this article.

SUMMARY

By mimicking mechanotransductive processes in cells by stress-induced cryptic site exhibition, we introduced here a new strategy to achieve fully reversible mechanoresponsive surfaces. Our strategy is based on embedding ligands into PEG brushes. By stretching the substrate, the ligands become accessible to proteinic receptors. Returning to the nonstretched state, the receptors are expelled from the PEG brush, assuring a full reversibility of the process. The validity of this concept was proven on the biotin/streptavidin system, the strongest noncovalent bond found in biology, on biotin/anti-biotin, and on the system RGD peptides with cells. We propose that the unbinding of streptavidin from biotin following the release of the mechanical constraints on the substrate is due to streptavidin conformational changes due to lateral constraints applied by PEG chains on the protein. This opens the route to developing substrates that allow modulating reversible chemical reactions by modifying conformations of enzymes anchored under stretching on the surface between grafted PEG chains simply by adapting the stretching degree of the substrate, a new technology of unknown consequences. By using artificial enzymes

based on adjoining guanidinium moieties on a Cu(II) complex of a tetraaza, one could create a substrate with carboxypeptidase A features.[21] The accessibility of proteins from the solution to the enzymatic site can then be modulated so that the enzymatic activity of the surface becomes modulated through the stretching degree. From a more applicative point of view, we envision using this technology in tissue engineering as mentioned above. We also envision using it for protein separation through the His-tag technology where proteins of interest, carrying either a C- or N-terminal histidine (His) tag, out of a complex protein solution can attach to the surface in the stretched state and can be released simply by unstretching the substrate. The interaction would take place through Ni^{2+} immobilized by chelation to nitrilotriacetic acid (NTA) anchored on the substrate in place of the PEG-biotin moieties. Finally, one can remark that cryptic sites can also be exposed reversibly by embedding them in a brush of polymers presenting a lower critical solution temperature. This led to the development of thermoresponsive systems allowing for cultured cell-detachable substrates for tissue engineering[22] and chromatographic matrices where proteins are force-released by temperature change.[23] Our cryptic site mechanoresponsive system allows achieving similar effects, yet with a totally different stimulus: mechanics instead of temperature. Whereas temperature appears as a natural parameter to control molecular binding, mechanics only recently has been shown to be able to act on chemistry. In addition, mechanics allows modulating ligand densities which could be of widespread use in tissue engineering, where cell fate appears sensitive to adhesion ligand density. This could allow, in particular, one to vary the adhesion ligand density during the cell adhesion process, a tool that opens new exciting perspectives in studies of cell fate guided by their environment.

MATERIALS AND METHODS

Materials. Silicone substrates were molded by Statice Santé SAS (France) using MED-4750 from NuSil Silicone Technology LCC (Carpinteria, California, USA). Briquettes of maleic anhydride (99.5% purity) were provided by Prolabo and were used as received. *N*-(3-Dimethylaminopropyl)-*N*′-ethylcarbodiimide hydrochloride (EDC), hydroxysulfosuccinimide sodium salt (sulfo-NHS), fluorescein-functionalized streptavidin (streptavidin-FITC), bovine serum albumin, dichloromethane (99%+), acetonitrile (HPLC grade), triphenylphosphine, 2,2′-(ethylenedioxy)bis-(ethylamine) (98%), biotin (99%), DMF, THF, and MeOH (99%+) were purchased from Aldrich Chemical Co. Fluorescein-functionalized anti-biotin IgG (antibody-FITC) was purchased from Jackson ImmunoResearch. Peptide (D)FKRGD was obtained from Proteogenix (Oberhausbergen, France). α-Methoxy-ω-hydroxy polyethylene glycol (PEG-MW 2000 Da) and α-methoxy-ω-amino polyethylene glycol (PEG-MW 750 Da and PEG-MW 5000 Da) were purchased from Iris Biotech GmbH. Methanesulfonyl chloride (98%) and sodium azide (99%) were purchased from Alfa Aesar. Triethylamine (99%) was purchased from Acros. BOP was purchased from Novabiochem. Chloroform-*d* was purchased from Euriso-top.

Synthesis details of 5-(2-oxohexahydrothieno[3,4-*d*]imidazol-4-yl)-pentanoic acid 2-[2-aminoethoxy)ethoxy]ethylamide and α-methoxy-ω-amino polyethylene glycol are found in Supporting Information.

All reactants and solvents were used as received, except dichloromethane, which was distilled over CaH_2 prior to use.

Elaboration of the Stretchable Filler-Free PDMS Surface. *Preparation of the Filler-Free PDMS Resin.* The filler-free PDMS resins were prepared from a linear dimethylvinylmethylsiloxane copolymer (M_n = 28 000, ABCR, AB109358, Germany) under nitrogen. The reaction between vinyl groups forming a cross-linked PDMS network was initiated by addition of (i) 0.9% (w/w) tetrakis-(dimethylsiloxy)silane (97%, ABCR, AB11396, Germany) to the linear PDMS and (ii) 2 drops of 0.2 vol % solution of three platinum divinyltetramethyldisiloxane (ABCR, AB 108773, Germany) diluted in heptane.

Plasma Treatment of the Commercial Filler Containing PDMS Substrate. Plasma surface modifications were conducted using a radio frequency (rf) inductive coupling plasma reactor (Plassys MDS 130) consisting of a cylindrical glass chamber (14.5 cm diameter and 5.5 L volume) enclosed in a Faraday cage. In the Ar plasma reactions, the PDMS substrates from Statice Santé, with approximate dimensions of 15 × 45 × 0.2 mm, were placed into the plasma chamber at 27 cm from the gas inlet. The reactor was evacuated to 1×10^{-3} mbar, followed by purging with Ar gas to the desired experimental pressure, typically 1 mbar. At this point, rf radiations were turned on (60 W) to induce plasma reactions. Upon completion (*i.e.*, 60 s of exposition time), the rf generator was switched off. Then, the system was vented up to atmospheric pressure, and the sample was immediately removed from the reactor and stocked under nitrogen by minimizing exposure with air (less than 20 s).

Preparation of the Stretchable Filler-Free PDMS Surface. The filler-free PDMS resin was molded against the Ar plasma-treated PDMS surface using a homemade Teflon matrix (always under nitrogen). Then the PDMS/PDMS sample was removed from the Teflon matrix, and the cross-linking reactions were accomplished by post-curing the PDMS/PDMS sample successively at 60 °C during 24 h and at 160 °C during 24 h.

Functionalization of the Stretchable Filler-Free PDMS Surface with Anhydride Groups by Plasma Polymerization. *Maleic Anhydride Plasma Polymerization.* The plasma reactor consisted of an electrodeless cylindrical glass reactor (6 cm diameter, 680 cm^3 volume, base pressure 5×10^{-4} mbar, and leak rate better than 1.0×10^{-10} kg s^{-1}) enclosed in a Faraday cage. The chamber was fitted with a gas inlet, a Pirani pressure gauge, a two-stage rotary pump (Edwards) connected to a liquid nitrogen cold trap, and an externally wound copper coil (4 mm diameter, 5 turns). All joints were grease-free. An L-C matching network (Dressler, VM 1500 W-ICP) was used to match the output impedance of a 13.56 MHz rf power supply (Dressler, Cesar 133) to the partially ionized gas load by minimizing the standing wave ratio of the transmitted power. During electrical pulsing, the pulse shape was monitored with an oscilloscope, and the average power $\langle P \rangle$ delivered to the system was calculated using the following expression: $\langle P \rangle = P_p[t_{on}/(t_{on} + t_{off})]$, where P_p is the average continuous wave power output and $t_{on}/(t_{on} + t_{off})$ is defined as the duty cycle. Prior to each experiment, the reactor was cleaned by scrubbing with detergent, rinsing in propan-2-ol, oven drying, followed by a 30 min high-power (60 W) air plasma treatment. The system was then vented to air, and a stretched filler-free PDMS sheet (5 cm × 1.5 cm) was placed in the chamber (8 cm from the gas inlet) followed by evacuation back down to initial pressure.

Plasma polymerization of maleic anhydride was carried out as follows: maleic anhydride (Prolabo, 99.5% purity) was ground into a fine powder and loaded into a stoppered glass gas delivery tube. Subsequently, maleic anhydride vapor was introduced into the reaction chamber at a constant pressure of 0.2 mbar and with a flow rate of approximately 1.6×10^{-9} kg s^{-1}. At this stage, the plasma was ignited and ran for 6 min. The optimum deposition conditions correspond to power output of 15 W, pulse on-time of 25 μs, and off-time of 1200 μs.

Upon completion of deposition, the rf generator was switched off, and the monomer feed was allowed to continue to flow through the system for a further 2 min prior to venting up to atmospheric pressure.

Hydrolysis of the Maleic Anhydride Plasma Polymer Films. Hydrolysis of the maleic anhydride plasma polymer films was realized by immersing the freshly modified PDMS substrates in deionized water for 24 h.

Covalent Grafting of Amine-Functionalized Molecules on Plasma Polymer. Hydrolyzed maleic anhydride plasma polymer substrates were soaked in a pH 5 phosphate buffer solution containing EDC (20 mg mL^{-1}) and NHS (2 mg mL^{-1}) coupling agents. After 45 min incubation at 4 °C, the activated surfaces were directly immersed in a phosphate buffered saline (PBS) solution at pH 7.4, containing amines. Amino-PEGs (750, 2000, and 5000) (20 mg mL^{-1}) were allowed to react for 12 h at 60 °C. The same procedure was followed for amino-PEG_2biotin or peptide (D)FKRGD grafting except that the reaction was conducted at room temperature during 6 h.

At the end of the coupling reactions, functionalized substrates were rinsed alternatively in acidic, basic, and 1 M KCl solutions and kept at 4 °C in deionized water prior to use.

Protein Adsorption. Surfaces were brought into contact with a streptavidin-FITC or bovine serum albumin or anti-biotin IgG antibody-FITC solution (0.1 mg mL^{-1} in PBS) for 5 min and rinsed three times for 3 min in PBS. Adsorption was measured in PBS by epifluorescence microscopy (Olympus BX51) and using 2 s as exposition time. For each sample, five fluorescence micrographs were acquired at different locations. Fluorescence micrographs were analyzed using the ImageJ 1.43s software (National Institute of Mental Health, Bethesda, Maryland). The relative adsorption corresponds to the difference between the fluorescence intensity (i) measured after adsorption and rinsing steps and (ii) the background fluorescence signal measured prior to adsorption. Subsequently, the substrate was elongated at 60% strain, and the same procedure was used to measure the additional adsorption.

Cell Culture, Staining, and Observation. Experiments were performed with immortalized human F/STRO-1+ A osteoprogenitor cells kindly provided by P. Marie (Hôpital Lariboisière, Paris, France).[24] Cells were cultured in Iscove medium complemented with 2 mM of L-glutamine, 0.1 mg mL^{-1} of streptomycine, and 100 U mL^{-1} of penicillin from Sigma (France) and 10% (v/v) of fetal bovine serum (FBS) from VWR International (France). When cells had reached confluence, nuclei of cells were labeled with a 2 μM solution of Hoechst (Sigma-Aldrich) in complete Iscove medium during 2 h. A solution of trypsin-EDTA (Sigma-Aldrich) was used to remove cells from the culture dish. Cells were then incubated 15 min in a solution of Iscove medium with 5 μM of CFDA,SE for cell body labeling (Life Technologies Invitrogen, France). After rinsing, cells were seeded at a concentration of 10^4 cells/cm^2 on the different samples. Another batch of F/STRO-1+ A cells was transfected with talin-GFP (Life Technologies Invitrogen). Talin-GFP constructs are embedded in baculoviruses to allow the cell transfection and the synthesis of a fluorescent talin by the cell. Cells were incubated 16 h with a rate of 50 baculovirus particles per cell. Transfected cells were seeded on stretched PEG-RGD substrates and cultured at 37 °C and 5% of CO_2.

The behavior of cells on samples was observed under a LSM700 confocal microscope (Zeiss, France) with a specific chamber to keep cells in optimal conditions (5% CO_2 and 37 °C). An immersion objective was used to watch living cells in the culture dish filled with medium. Cell adhesion was tested by flowing medium with a micropipet in the culture dishes. Micrographs were analyzed with Zen software (Zeiss, France). Image analysis was done thanks to ImageJ 1.43s software (National Institute of Mental Health, Bethesda, Maryland).

Contact Angle Measurements. Contact angle measurements were carried out using a video capture apparatus goniometer Krüss (DSA100) with 2 μL high-purity water drops. Advancing contact angle values were determined by increasing the sessile drop volume. Measurements were made on both sides of the drop and were averaged. All results are the average of five contact angle values.

X-ray Photoelectron Spectroscopy Analysis. X-ray photoelectron spectroscopy (XPS) spectra were recorded with a LEYBOLD LHS-11 spectrometer equipped with a concentric hemispherical analyzer. The incident radiation used was generated by a nonmonochromatic Mg Kα X-ray source (1253.6 eV) operating at 330 W (11 kV; 30 mA). Photoemitted electrons were collected at a takeoff angle of 90° from the substrate, with electron detection in the constant analyzer energy mode. Survey spectrum signal was recorded with a pass energy of 100 eV, and for high-resolution spectra (C 1s, O 1s, and Si 2p), pass energy was set to 20 eV. The analyzed surface area was approximately 8 mm^2, and the base pressure in the analysis chamber during experimentation was about 10^{-9} mbar. Charging effects on these isolating samples were not compensated by the usage of a flood gun. The spectrometer energy scale was calibrated using the Ag $3d^{5/2}$, Au $4f^{7/2}$, and Cu $2p^{3/2}$ core level peaks, set, respectively, at binding energies of 368.2, 84.0, and 932.7 eV. Peak fitting was made with mixed Gaussian−Lorentzian (30−70%) components with equal full width at half-maximum (fwhm) using CasaXPS software. The surface composition expressed in atom percentage was determined using integrated peak areas of each component and takes into account the transmission factor of the spectrometer, mean free path, and Scofield sensitivity factors of each atom (C 1s, 1.00; O 1s, 2.85; Si 2p, 0.87; and N 1s, 1.80).

Atomic Force Microscopy. AFM experiments were carried out using MFP3D-BIO instrument (Asylum Research Technology, Atomic Force F&E GmbH, Mannheim, Germany). Silicon nitride cantilevers of conical shape were purchased from Veeco (MLCT-AUNM, Bruker Nano AXS, Palaiseau, France). The spring constants of the cantilevers measured using thermal noise method[25] were found to be 9.6 pN nm^{-1}, and the curvature radius of the AFM tips is about 20 nm. Cantilever calibration was performed over a piece of fresh silicon substrate before manipulations on PDMS films, and the maximal loading force was about 0.5 nN for a pulling speed of 2000 nm s^{-1} in order to keep *the same contact area and contact geometry* between AFM tips and each sample. Force−displacement curves were acquired at a pH value of 7.4 and at room temperature. AFM tips were functionalized with streptavidin according the protocol published by Hinterdorfer *et al.*[26] Interaction forces are calculated following Hooke's low: $F = K_c \cdot \Delta z$, where K_c (pN nm^{-1}) is the cantilever spring constant and Δz (nm) is the cantilever deflection (bending of the cantilever from its equilibrium position). The rupture force of the streptavidin−biotin complex was measured at a retraction rate of 2000 nm s^{-1}. Maps of adhesion forces were obtained by recording a grid map of 10 × 10 force curves three times at six different locations (corresponding to scanned area of 20 μm × 20 μm) of the film surface.

Stretching Device. A homemade stretching device enabled elongation of the silicone substrates directly under a confocal microscope. The stretching degree is defined by the parameter $\alpha = (L - L_0)/L_0$, where L_0 and L correspond, respectively, to the initial and to the stretched length of the silicone sheet. The stretching motion is achieved by a precision electric motor at a velocity of 0.27 mm/s.

Conflict of Interest: The authors declare no competing financial interest.

Acknowledgment. The authors gratefully acknowledge the financial support from Region Alsace in France, from the French National Research Agency (*Biostretch* project), from the ci-FRC of Strasbourg and from the IRTG.

Supporting Information Available: Experimental details about the synthesis of the grafted molecules. Also given are Figures S1−S10. This material is available free of charge *via* the Internet at http://pubs.acs.org.

REFERENCES AND NOTES

1. Caruso, M. M.; Davis, D. A.; Shen, Q.; Odom, S. A.; Sottos, N. R.; White, S. R.; Moore, J. S. Mechanically-Induced Chemical Changes in Polymeric Materials. *Chem. Rev.* **2009**, *109*, 5755–5798.

2. Liang, J.; Fernandez, J. M. Mechanochemistry: One Bond at a Time. *ACS Nano* **2009**, *3*, 1628–1645.
3. Davis, D. A.; Hamilton, A.; Yang, J. L.; Cremar, L. D.; Van Gough, D.; Potisek, S. L.; Ong, M. T.; Braun, P. V.; Martinez, T. J.; White, S. R. Force-Induced Activation of Covalent Bonds in Mechanoresponsive Polymeric Materials. *Nature* **2009**, *459*, 68–72.
4. Piermattei, A.; Karthikeyan, S.; Sijbesma, R. P. Activating Catalysts with Mechanical Force. *Nat. Chem.* **2009**, *1*, 133–137.
5. Halford, B. Tugging on Molecules. *Chem. Eng. News* **2012**, *90*, 55–57.
6. del Rio, A.; Perez-Jimenez, R.; Liu, R. C.; Roca-Cusachs, P.; Fernandez, J. M.; Sheetz, M. P. Stretching Single Talin Rod Molecules Activates Vinculin Binding. *Science* **2009**, *323*, 638–641.
7. Gao, M.; Craig, D.; Vogel, V.; Schulten, K. Identifying Unfolding Intermediates of FN-III10 by Steered Molecular Dynamics. *J. Mol. Biol.* **2002**, *323*, 939–950.
8. Vogel, V. Mechanotransduction Involving Multimodular Proteins: Converting Force into Biochemical Signals. *Annu. Rev. Biophys. Biomol. Struct.* **2006**, *35*, 459–488.
9. Mertz, D.; Vogt, C.; Hemmerle, J.; Mutterer, J.; Ball, V.; Voegel, J. C.; Schaaf, P.; Lavalle, P. Mechanotransductive Surfaces for Reversible Biocatalysis Activation. *Nat. Mater.* **2009**, *8*, 731–735.
10. Davila, J.; Chassepot, A.; Longo, J.; Boulmedais, F.; Reisch, A.; Frisch, B.; Meyer, F.; Voegel, J. C.; Mésini, P. J.; Senger, B.; *et al.* Cyto-Mechanoresponsive Polyelectrolyte Multilayer Films. *J. Am. Chem. Soc.* **2012**, *134*, 83–86.
11. Mertz, D.; Vogt, C.; Hemmerle, J.; Debry, C.; Voegel, J. C.; Schaaf, P.; Lavalle, P. Tailored Design of Mechanically Sensitive Biocatalytic Assemblies Based on Polyelectrolyte Multilayers. *J. Mater. Chem.* **2011**, *21*, 8324–8331.
12. Genzer, J.; Efimenko, K. Creating Long-Lived Superhydrophobic Polymer Surfaces through Mechanically Assembled Monolayers. *Science* **2000**, *290*, 2130–2133.
13. Geissler, A.; Vallat, M. F.; Fioux, P.; Thomann, J. S.; Frisch, B.; Voegel, J. C.; Hemmerlé, J.; Schaaf, P.; Roucoules, V. Multifunctional Stretchable Plasma Polymer Modified PDMS Interface for Mechanically Responsive Materials. *Plasma Processes Polym.* **2010**, *7*, 64–77.
14. Emoto, K.; Harris, J. M.; Van Alstine, J. M. Grafting of Poly(ethyleneglycol) Epoxide to Amino Derivatized Quartz: Effect of Temperature on pH on Grafting Density. *Anal. Chem.* **1996**, *68*, 3751–3757.
15. Kingshott, P.; Thissen, H.; Griesser, H. J. Effects of Cloud-Point Grafting, Chain Length, and Density of PEG Layers on Competitive Adsorption of Ocular Proteins. *Biomaterials* **2002**, *23*, 2043–2056.
16. Teulon, J.-M.; Delcuze, Y.; Odorico, M.; Chen, S. W.; Parot, P.; Pellequer, J. L. Single and Multiple Bonds in (Strept)-Avidin−Biotin Interactions. *J. Mol. Recognit.* **2010**, *24*, 490–502.
17. Friquet, B.; Chaffotte, A. F.; Djavadi-Ohaniance, L.; Goldberg, M. E. Measurements of the True Affinity Constant in Solution of Antigen-Antibody Complexes by Enzyme-Linked Immunosorbent Assay. *J. Immunol. Methods* **1985**, *77*, 305–319.
18. Pierschbacher, M. D.; Ruoslahti, E. The Cell Attachment Activity of Fibronectin Can Be Duplicated by Small Fragments of Molecules. *Nature* **1984**, *309*, 30–33.
19. Ruoslahti, E. RGD and Other Recognition Sequences for Integrins. *Annu. Rev. Cell Dev. Biol.* **1996**, *12*, 697–715.
20. Smith, M. L.; Gourdon, D.; Little, W. C.; Kubow, K. E.; Eguiluz, R. A.; Luna-Morris, S.; Vogel, V. Force-Induced Unfolding of Fibronectin in the Extracellular Matrix of Living Cells. *PLoS Biol.* **2007**, *5*, 2243–2254.
21. Yin, Y.; Dong, Z.; Luo, Q.; Liu, J. Biomimetic Catalysts Designed on Macromolecular Scafolds. *Prog. Polym. Sci.* **2012**, *37*, 1476–1509.
22. Yamada, N.; Okano, T.; Sakai, H.; Karikusa, F.; Sawasaki, Y.; Sakurai, Y. Thermoresponsive Polymeric Surfaces—Control of Attachment and Detachment of Cultured-Cells. *Makromol. Chem., Rapid Commun.* **1990**, *11*, 571–576.
23. Yoshizako, K.; Akiyama, Y.; Yamanaka, H.; Shinohara, Y.; Hasegawa, Y.; Carredano, E.; Kikuchi, A.; Okano, T. Regulation of Protein Binding toward a Ligand on Chromatographic Matrixes by Masking and Forced-Releasing Effects Using Thermoresponsive Polymer. *Anal. Chem.* **2002**, *74*, 4160–4166.
24. Oyajobi, B. O.; Lomri, A.; Hott, M.; Marie, P. J. Isolation and Characterization of Human Clonogenic Osteoblast Progenitors Immunoselected from Fetal Bone Marrow Stroma Using STRO-1 Monoclonal Antibody. *J. Bone Miner. Res.* **1999**, *14*, 351–361.
25. Hutter, J. L.; Bechhoefer, J. Calibration of Atomic-Force Microscope Tips. *Rev. Sci. Instrum.* **1993**, *64*, 1868–1873.
26. Hinterdorfer, P.; Dufrene, Y. F. Detection and Localization of Single Molecular Recognition Events Using Atomic Force Microscopy. *Nat. Methods* **2006**, *3*, 347–355.